Computers, Materials & Continua CMC, vol.64, no.1, pp.145-160, 2020

A Novel Technique for Estimating the Numerical Error in Solving the Helmholtz Equation

Kue-Hong Chen[1, *] and Cheng-Tsung Chen[2, 3]

Abstract: In this study, we applied a defined auxiliary problem in a novel error estimation technique to estimate the numerical error in the method of fundamental solutions (MFS) for solving the Helmholtz equation. The defined auxiliary problem is substituted for the real problem, and its analytical solution is generated using the complementary solution set of the governing equation. By solving the auxiliary problem and comparing the solution with the quasianalytical solution, an error curve of the MFS versus the source location parameters can be obtained. Thus, the optimal location parameter can be identified. The convergent numerical solution can be obtained and applied to the case of an unavailable analytical solution condition in the real problem. Consequently, we developed a systematic error estimation scheme to identify an optimal parameter. Through numerical experiments, the optimal location parameter of the source points and the optimal number of source points in the MFS were studied and obtained using the error estimation technique.

Keywords: Error estimation, auxiliary problem, optimal parameter, method of fundamental solutions, complementary solution, quasianalytical solution.

1 Introduction

Meshless methods have become popular and attractive alternatives to traditional mesh or mesh reduction methods over the past decades. Meshless methods have been successfully applied to several major types of engineering problems, as described in the literature [Atluri and Zhu (1998); Atluri and Shen (2002); Atluri (2004)]. The method of fundamental solutions (MFS) is an intuitive meshless technique for obtaining numerical solutions [Chen, Chang, Chen et al. (2002); Chen, Chen, Chen et al. (2004); Reutskiy (2005); Liu (2008); Alves (2009); Karageorghis and Lesnic (2009); Liu and Sarler (2013); Zhang, Li, Wei et al. (2013)]. However, the MFS has several drawbacks that impair its computational ability and restrict its applicability to practical problems [Young, Chen and Lee (2005, 2006); Young, Chen, Chen et al. (2007); Chen, Chen and Kao (2008); Young, Chen, Liu et al. (2009);

[1] Department of Civil Engineering, National Ilan University, Ilan, 26047, Taiwan.

[2] Department of Civil Engineering, Yancheng Institute of Technology, Yancheng, 224051, China.

[3] Center for Innovative Research on Aging Society, National Chung Cheng University, Chia-yi, 621301, Taiwan.

[*] Corresponding Author: Kue-Hong Chen. Email: khc6177@niu.edu.tw.

Received: 19 October 2019; Accepted: 14 January 2020.

Chen, Lin and Wang (2011); Chen and Gu (2012)]. Notably, the location parameter is crucial for the precision of a solution [Chen and Gu (2012)]. Some types of uncertainty occur in the MFS; we have no criteria for determining the applicable location of the source points outside the problem domain [Young, Chen and Lee (2005)]. A specific characteristic of the MFS is the wide freedom of choice it enables in selecting source points. This distance between the source and collocation points may lead to an ill-defined influence matrix, causing the behavior to lead to a potentially unstable solution. Different source locations may yield accurate or poor results [Young, Chen and Lee (2006)]. Consequently, the shape parameter for the source point locations substantially influences the stability and convergence rate of the solution [Chen, Kao, Chen et al. (2006)].

The MFS is successful because of its excellent performance and high convergent order that results from its exponential error convergence rate. Numerical tests described in the literature [Reutskiy (2005)] indicate that the MFS performs optimally concerning to the accuracy, stability, efficiency, memory requirement, and simplicity in implementation. Because the optimal location parameter in the conventional MFS can be detected, it can be considered a highly efficient and accurate algorithm beyond the reach of traditional methods [Song and Chen (2009)]. Theoretically, the radius of the enclosing circle on which the source points of fundamental solutions are distributed should be as large as possible [Huang, Lee and Cheng (2007)]. The aforementioned discussion of the optimal parameter is based on infinite precision computation. Infinite precision computation, the precision is limited to a double-precision that limits the optimal parameter value. Therefore, to determine the optimal parameter in the MFS, we developed an error estimation technique [Chen and Chen (2014)] to estimate the numerical error in different location parameters.

We developed an alternative error estimation technique for detecting the optimal parameter in the MFS [Chen and Chen (2014)]. This technique predicts the applicable region of the source point distribution without deriving an analytical solution. The technique estimates the error magnitude, which is crucial for comparison with a different number of source points or a different parameter. By adopting the optimal distance between the source and field points in the MFS, the convergent result can be obtained and used in the case of an unavailable analytical solution condition. A quasianalytical solution similar to the real analytical solution is simulated to substitute the real analytical solution by employing the complementary solution set. The error curves are derived by comparing the computed numerical solution with the quasianalytical solution. Both the optimal parameter and the optimal number of source point locations can be determined from the obtained error curves. Subsequently, a systematic error estimation scheme is constructed to determine the optimal parameter in the MFS. The error estimation technique was successfully applied to solve the Laplace equation [Chen and Chen (2014)], therefore, we extend it to solve the Helmholtz equation in this study.

2 Problem statement and solution method

2.1 Problem statement

For a boundary value problem for a two-dimensional (2D) bounded domain, the governing equation (GE) and mixed-type boundary conditions (BCs) for the interior Helmholtz problem are as follows:

$$\nabla^2 u(x) + k^2 u(x) = 0, x \in D \tag{1}$$

$$u(x) = \overline{u}(x), x \in B_1 \tag{2}$$

$$t(x) = \frac{\partial u(x)}{\partial n_x} = \overline{t}(x), x \in B_2 \tag{3}$$

where ∇^2 is the Laplace operator, $u(x)$ is the potential function, k is the wavenumber, D is the domain of the problem, and $B = B_1 \bigcup B_2 = \partial D$ denotes the whole boundary of the domain D. $\overline{u}(x)$ of B_1 is the essential boundary (Dirichlet boundary) in which the potential is prescribed. $\overline{t}(x)$ of B_2 is the natural boundary (Neumann boundary) in which the normal derivative of the potential in the n_x direction is specified.

2.2 Solution method

By employing the radial basis function concept, the representation of the solution in Eq. (1) can be approximated in terms of a set of interpolation functions, as follows:

$$u(x_i) = \sum_{j=1}^{N} c_j \phi_j(x_i, s_j) \tag{4}$$

Here, $\phi_j(x_i, s_j)$ can be selected using the fundamental solution of the 2D Helmholtz equation, i.e., $U_j(x_i, s_j)$, and as follows:

$$\phi_j(x_i, s_j) = U(x_i, s_j) = \frac{-i\pi H_0^{(1)}\left(kr_{ij}\right)}{2} \tag{5}$$

where r is the distance between the j^{th} source point (singularity) s_j and the i^{th} observation point x_i, k is the wavenumber, $H_n^{(1)}(kr) = J_n(kr) + iY_n(kr)$ is the n^{th} order Hankel function of the first type, in which J_n is the n^{th}-order Bessel function, and Y_n is the n^{th}-order Bessel function of the second type.

The N source points are located outside the domain D. The potential and it's derivative in the normal direction (flux) can be approximated in terms of the linear algebra system, represented as follows:

$$\begin{bmatrix} U_1 \\ U_2 \end{bmatrix} c = \begin{Bmatrix} \overline{u}_1 \\ \overline{u}_2 \end{Bmatrix} \tag{6}$$

$$\begin{bmatrix} L_1 \\ L_2 \end{bmatrix} c = \begin{Bmatrix} \overline{t}_1 \\ \overline{t}_2 \end{Bmatrix} \tag{7}$$

After imposing the corresponding BCs, the resulting system of linear equations can be expressed in the matrix form of a linear combination of Eqs. (6) and (7), as follows:

$$\begin{bmatrix} U_1 \\ L_2 \end{bmatrix} c = \begin{Bmatrix} \overline{u}_1 \\ \overline{t}_2 \end{Bmatrix} \tag{8}$$

We can derive the unknown coefficient c_j of the linear algebra system in Eq. (8) using the linear algebraic solver as follows:

$$c = \begin{bmatrix} U_1 \\ L_2 \end{bmatrix}^{-1} \begin{Bmatrix} \overline{u}_1 \\ \overline{t}_2 \end{Bmatrix} \tag{9}$$

We can derive the unknown coefficient c_j of the linear algebra system in Eq. (9) by using the linear algebraic solver. Notably, the location of the source points (shape parameters) critically affects the accuracy of the MFS and distance between the fictitious and physical boundaries, which are defined by *d* and must be considered deliberately. To overcome the aforementioned shortcoming, we developed an optimal parameter estimation technique to derive the applicable region, as described in Section 3.

3 Novel error estimation technique

The formula for obtaining the real analytical solution to obtain the error norm in the realistic engineering problem is difficult to derive. To overcome this drawback, an alternative problem is defined.

3.1 Auxiliary problem definition

3.1.1 Definition of GE and BC types and contour

The GE and BC types and geometric contours in the new problem are identical to those in the original problem.

3.1.2 Quasianalytical solution production

In this study, the potential of a newly defined problem, $\phi(x)$, is specified by the complementary solution set, which is the complete set. The quasianalytical solution $u^{\text{q-a}}(x)$ to the new problem at an arbitrary point x in the domain is the linear combination of the complementary solutions, as follows:

$$u^{\text{q-a}}(x) = \sum_{j=1}^{M} v_j \phi_j(x), x \in D \tag{10}$$

The complementary solutions are selected as the $\phi_j(x)$ that satisfies the governing Eq. (1). M is the total number of complete functions and v_j denotes the undetermined coefficient. The quasianalytical solutions for the Helmholtz equation are selected from the complete solution sets, expressed as follows:

$$\left\{ J_0(kr), J_m(kr)\cos m\varphi, J_m(kr)\sin m\varphi \right\} \text{ for } (m = 1, 2, \cdots) \tag{11}$$

where (r,φ) are polar coordinates. All the functions satisfy the governing Helmholtz equation in Eq. (1), indicated as follows:

$$\Delta\left[\phi_{(1)}(x)\right]=0,\Delta\left[\phi_{(2)}(x)\right]=0,\cdots,\Delta\left[\phi_{(M-1)}(x)\right]=0,\Delta\left[\phi_{(M)}(x)\right]=0 \tag{12}$$

where $\Delta=\nabla^2+k^2$. Because of the linear property of the differential equation operator in the GE, the potential $u^{\text{q-a}}(x)$ satisfies the GE, as follows:

$$\Delta\left[u^{\text{q-a}}(x)\right]=v_1\Delta\left[\phi_{(1)}(x)\right]+v_2\Delta\left[\phi_{(2)}(x)\right]+\cdots+v_{M-1}\Delta\left[\phi_{(M-1)}(x)\right]+v_M\Delta\left[\phi_{(M)}(x)\right]=0 \tag{13}$$

Notably, the potential, $u^q(x)$, in the newly defined problem is an exact solution because it satisfies GE (Eq. (13)).

3.1.3 Specified BCs

The two problems have the same boundary contour and BC type. The BC of the new problem is expressed as follows:

$$\bar{\bar{u}}(x)=\sum_{j=1}^{M}v_j\phi_j(x),x\in B_1 \tag{14}$$

Its derivative in the normal direction (flux) is expressed as follows:

$$\bar{\bar{t}}(x)=\frac{\partial\bar{\bar{u}}(x)}{\partial n_x}=\sum_{j=1}^{M}v_j\frac{\partial\phi_j(x)}{\partial n_x},\ x\in B_2 \tag{15}$$

where $\bar{\bar{u}}(x)$ and $\bar{\bar{t}}(x)$ are the known potential and its derivative, respectively. The boundary value in the new problem with the M number of collocation points is specified by the BC in the original problem. The boundary value in the new problem with the specified M points is the same as that in the original problem. The undetermined coefficient v_j can be determined by matching the original BC to a set of selected points (M number of points). Therefore, the analytical solution to the new problem is called the quasianalytical solution and is similar to the real analytical solution.

By implementing the MFS to solve the defined auxiliary problem, the numerical solution can be compared with the quasianalytical solution to obtain the error norm.

3.1.4 Error analysis between newly defined and original problems

The relationship between the real analytical solution $u^{\text{a}}(x)$ and quasianalytical solution $u^{\text{q-a}}(x)$ is expressed as follows:

$$u^{\text{a}}(x)=u^{\text{q-a}}(x)+R_n(x) \tag{16}$$

where $R_n(x)=\sum_{j=M+1}^{\infty}v_j\phi_j(x)$

The remainder function satisfies the GE, and its exponential convergence is expressed as follows:

$$\left\| R_n\left(x\right)\right\| = O\left(r^{-n}\right),\ r>1 \tag{17}$$

Therefore, the difference between the two space solvers is derived as follows:

$$\left\| u^{\mathrm{a}}(x) - u^{\mathrm{q\text{-}a}}(x)\right\| = \left\| R_n\left(x\right)\right\| = C\left(r^{-n}\right) \tag{18}$$

where C is a bounded constant.

3.2 Obtaining error magnitude in the defined auxiliary problem using root mean square error

The error in the numerical solution to the defined auxiliary problem is obtained using the root mean square (RMS) error, which is obtained by comparing the numerical solution with the quasianalytical solution, expressed as follows:

$$RMS = \sqrt{\frac{1}{n}\sum_{i=1}^{n}\left[\tilde{u}\left(x_i\right) - u^{\mathrm{q\text{-}a}}\left(x_i\right)\right]^2} \Bigg/ \sqrt{\frac{1}{n}\sum_{i=1}^{n}\left[u^{\mathrm{q\text{-}a}}\left(x_i\right)\right]^2} \tag{19}$$

where n is the number of field points and $\tilde{u}\left(x\right)$ is the numerical solution to the auxiliary problem solved by the MFS. Fig. 1 is a flow chart of the formulation for implementing the novel error estimation scheme. Through the error convergence analysis of the auxiliary problem, we can obtain the error curve. Based on the set criteria determined by the balance between computational cost and accuracy, we can obtain the optimal number of source points in the neighboring region of the corner in the error curve.

3.3 Obtaining the optimal field solution to the original problem

By adopting the obtained optimal parameter (d_{opt}) and the optimal number of source points (N_{opt}) described in the previous section, the optimal solution to the original problem can be obtained by implementing the MFS.

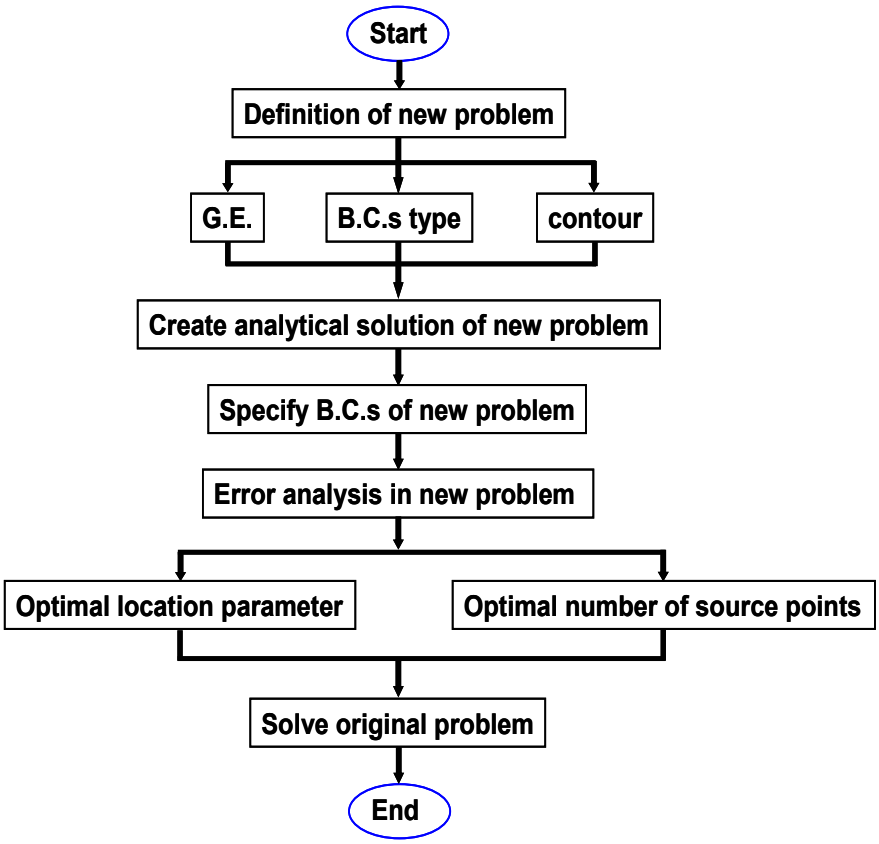

Figure 1: Flow chart of the new error estimation scheme

4 Numerical examples

Several problems subject to different BCs are considered for interior problems. We consider three cases for the interior problem to verify the accuracy of the new estimation technique and obtain the optimal parameter in the MFS. Although the new estimation technique does not require the aid of the analytical solution, we still provided the analytical solutions in the three cases to demonstrate the validity of the obtained error curve.

4.1 Case 1: circular case

A circular computational domain with a mixed-type BC is considered (Fig. 2) and the analytical solution to this problem is expressed as

$$\begin{cases} \overline{u} = e^{\frac{ik}{\sqrt{2}}(x+y)}, 0 \le \phi \le \pi \\ \overline{t} = \dfrac{ik}{\sqrt{2}}\left[\cos\phi + \sin\phi\right] e^{\frac{ik}{\sqrt{2}}(x+y)}, \pi \le \phi \le 2\pi \end{cases} \tag{20}$$

The analytical solution is expressed as follows:

$$u(x,y)=e^{\frac{ik(x+y)}{\sqrt{2}}} \tag{21}$$

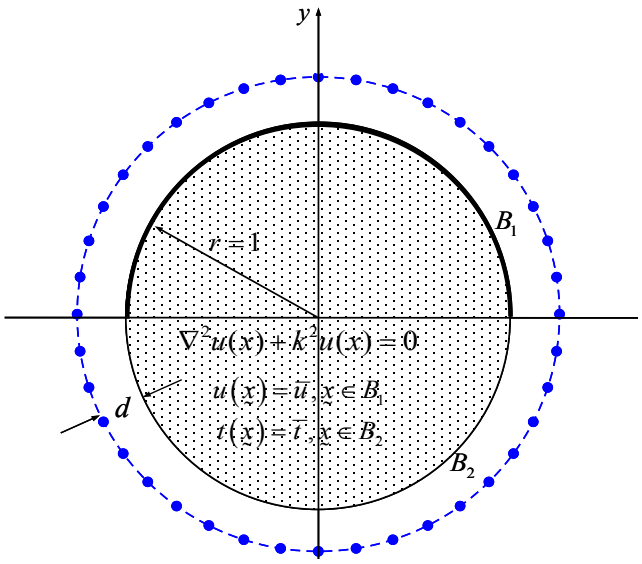

Figure 2: Problem sketch and source point distribution for Case 1

The wavenumber (k) of the solution equals $\sqrt{2}$. We implement the MFS to solve the defined auxiliary problem. To identify the optimal parameters $d_{\text{opt}}^{\text{q-a}}$ and $d_{\text{opt}}^{\text{a}}$, the RMS errors *vs*. the off-boundary distance (d) are plotted for various numbers of source points N (N=25, 28, 50) [Figs. 3(a-c)]. The error curves in Fig. 3 are used as indicators of error trends. The error curves in Figs. 3(a-c) demonstrate the optimal parameters $d_{\text{opt}}^{\text{q-a}}$ and $d_{\text{opt}}^{\text{a}}$, which are observed at the corners of the curves. The optimal parameter $d_{\text{opt}}^{\text{q-a}}$ approximating the optimal parameter $d_{\text{opt}}^{\text{a}}$ indicates that $d_{\text{opt}}^{\text{q-a}}$ is sufficiently accurate to be used for obtaining the convergent solution.

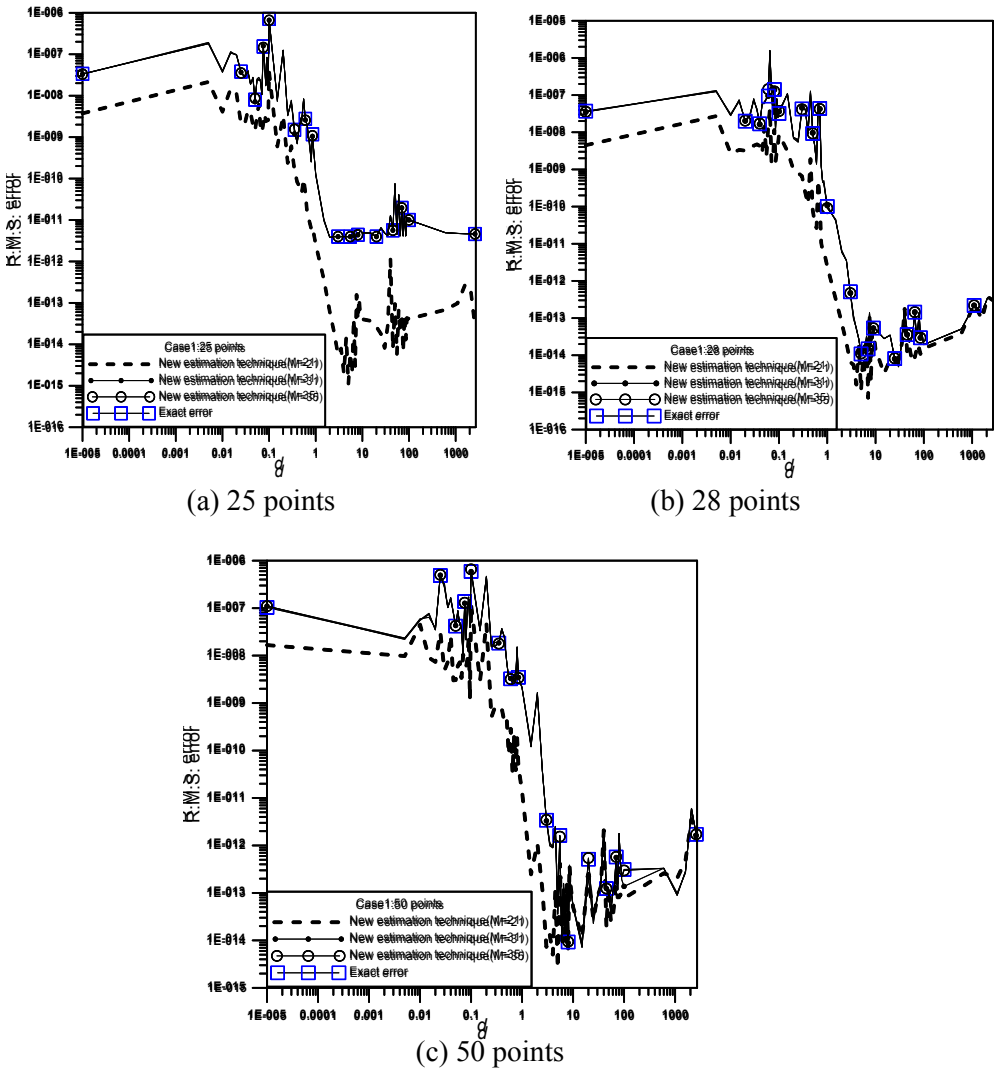

(a) 25 points (b) 28 points

(c) 50 points

Figure 3: Error analysis *vs.* location parameters: *d*, with different terms of the Trefftz basis; *M* for Case 1 of the interior problem; and *N*=(a) 25 points, (b) 28 points, and (c) 50 points

A plot of the RMS errors versus the different numbers of source points is displayed in Fig. 4. The RMS errors are obtained by adopting the optimal parameters ($d_{\text{opt}}^{\text{q-a}}$ and $d_{\text{opt}}^{\text{a}}$). The convergent result can be obtained when the number of source points equals 28. Therefore, we can obtain the optimal number of source points by employing the new error estimation technique.

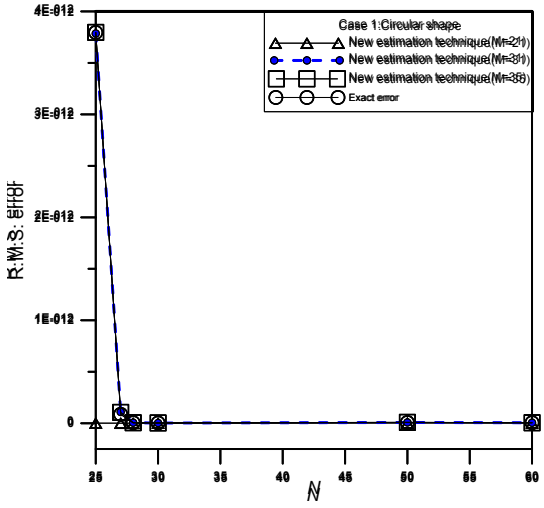

Figure 4: Root mean square error versus the number of source points N for Case 1

4.2 Case 2: square case

Case 2 considers a square domain subjected to Dirichlet and Neumann BCs, as illustrated in the Figs. 5(a) and 5(b), respectively, and their corresponding analytical solutions can be expressed as follows:

$$u(x,y)=\sin x\cos y,\ \ -0.5\le x\le 0.5,\ \ -0.5\le y\le 0.5. \tag{22}$$

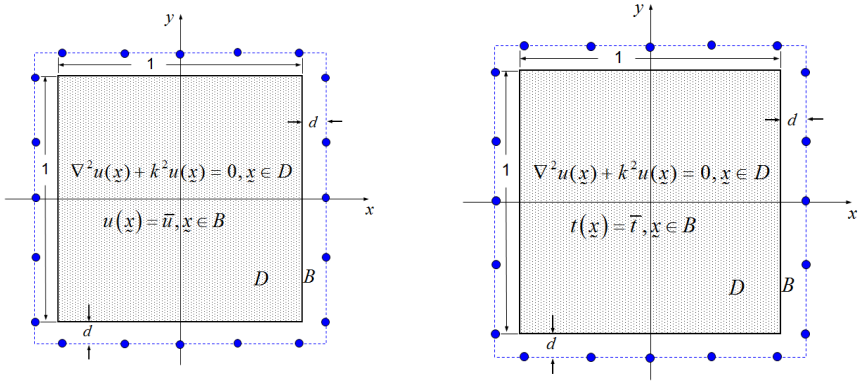

(a) Dirichlet BC (b) Neumann BC

Figure 5: Problem sketch and source point distribution of Case 2; (a) Dirichlet boundary condition (BC) and (b) Neumann BC

4.2.1 Case 2(a): Dirichlet BC

The Dirichlet BC on the boundary $\partial\Omega$ for a Dirichlet problem is expressed as follows:

$$u(x,y)=\sin x\cos y,\ \ x,y\in\partial\Omega \tag{23}$$

The RMS errors are plotted against different numbers of source points in Fig. 6, wherein the RMS errors are obtained by adopting the optimal parameters ($d_{\text{opt}}^{\text{q-a}}$ and $d_{\text{opt}}^{\text{a}}$). A convergent result can be obtained when the number of source points is over 24 points.

4.2.2 Case 2(b): Neumann BC

The Neumann BC on the boundary $\partial\Omega$ is specified as follows:

$$\frac{\partial u(x,y)}{\partial n_{\underset{\sim}{x}}} = \left(\cos x \cos y\right) n_x - \left(\sin x \sin y\right) n_y, \; x, y \in \partial\Omega \tag{24}$$

where $\left(n_x, n_y\right)$ is the component of the unit normal vector. Similar to the plot in the circular case, the RMS errors are plotted against different numbers of source points in Fig. 7, wherein the RMS errors are obtained by adopting the optimal parameters ($d_{\text{opt}}^{\text{q-a}}$ and $d_{\text{opt}}^{\text{a}}$). A convergent result can be obtained when the number of source points is over 24 points.

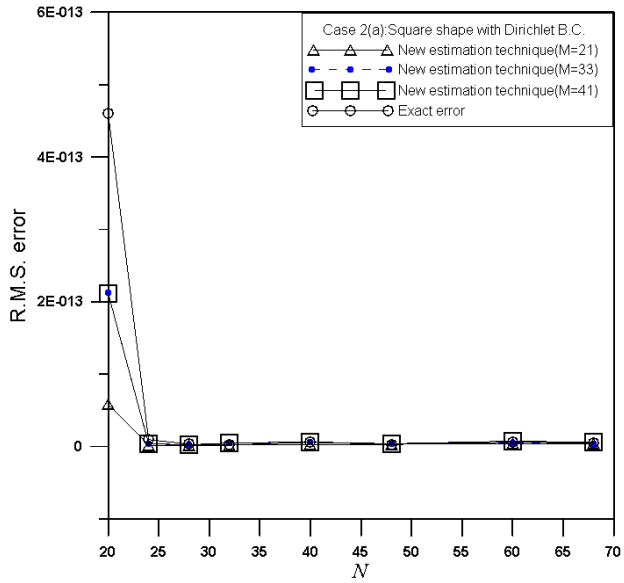

Figure 6: Root mean square error *vs. N* for Case 2(a)

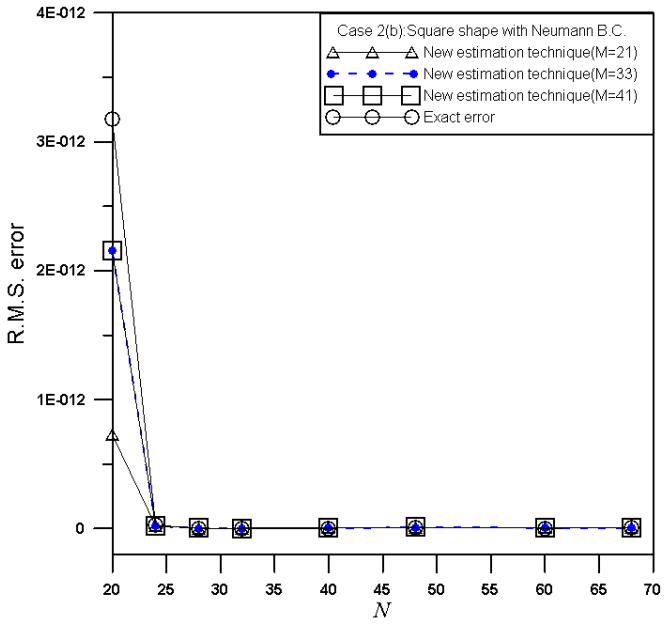

Figure 7: Root mean square error *vs.* N for Case 2(b)

4.3 Case 3: elliptical case

The BC on the boundary $\partial\Omega$ for a Dirichlet problem (Fig. 8) is described as follows:

$$\bar{u}(x,y)=\sin x\cos y,\ x,y\in\partial\Omega \tag{25}$$

Its analytical solution is given as follows:

$$u(x,y)=\sin x\cos y,\ -2\le x\le 2,\ -1\le y\le 1. \tag{26}$$

The RMS errors are plotted against different numbers of source points in Fig. 9, wherein the RMS errors are obtained by adopting the optimal parameters ($d_{\text{opt}}^{\text{q-a}}$ and $d_{\text{opt}}^{\text{a}}$). A convergent result of the new problem can be obtained when the number of source points is over 28 points.

Fig. 10(a) illustrates the analytical solution in the field in Eq. (26) and Fig. 10(b) demonstrates the field solution obtained by implementing the optimal parameter, $d_{\text{opt}}^{\text{q-a}}=8$, with 28 source points in the MFS. The results of Figs. 10(a) and 10(b) coincide.

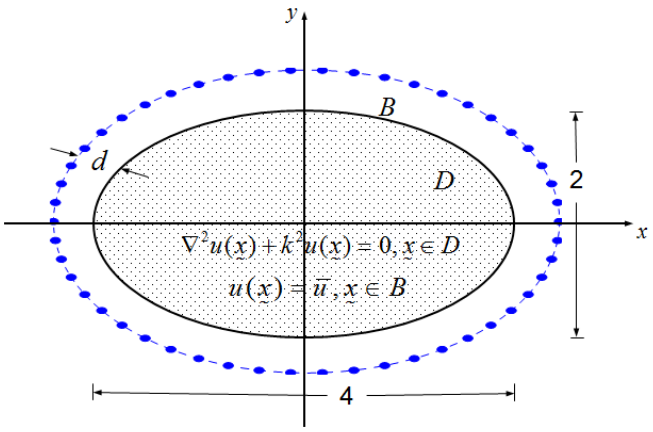

Figure 8: Problem sketch and source point distribution for Case 3

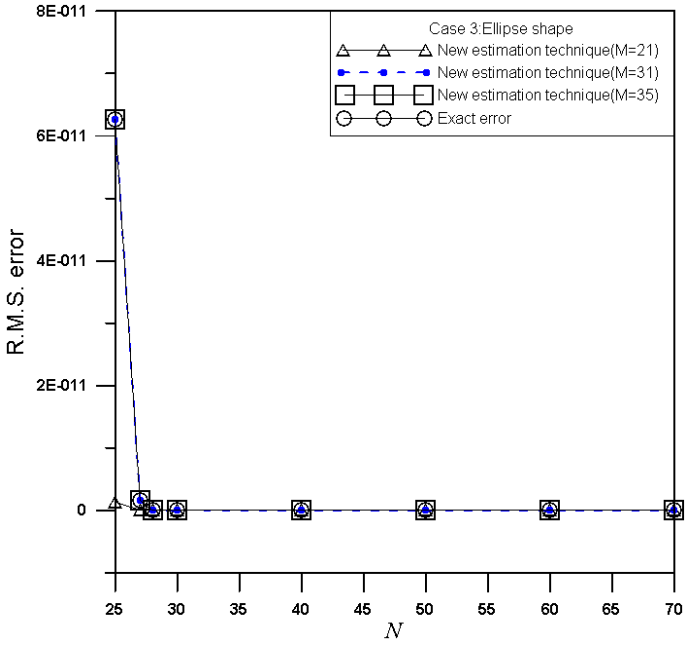

Figure 9: Root mean square error *vs. N* for Case 3

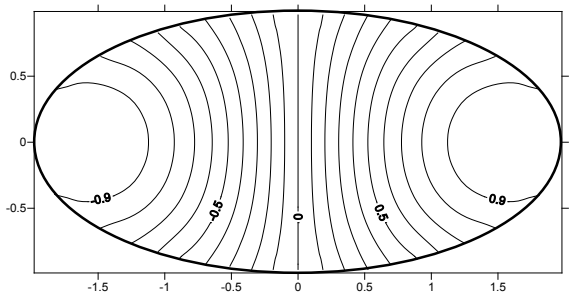

(a) Analytical solution

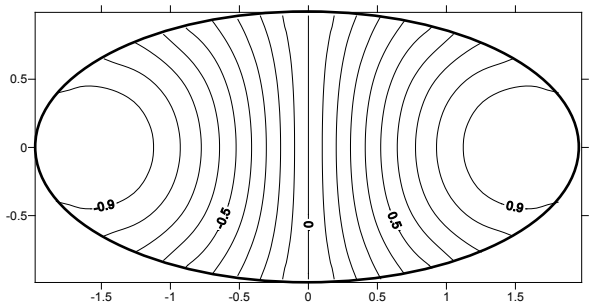

(b) MFS

Figure 10: Field solution for Case 3; (a) analytical solution and (b) method of fundamental solutions (MFS)

5 Conclusions

A new estimation technique was developed in this study. We successfully applied the estimation technique in the MFS to derive the optimal parameter without having an analytical solution. The technique was critical in maintaining the systematic characteristics of the MFS because of its excellent performance and high convergence order, because it has an exponential error convergence rate. The main disadvantage of using the MFS is that it raises a problem involving a perplexing fictitious boundary, which can be overcome by adopting the obtained optimal parameter. The convergence study of the cases yielded convergent results. The numerical results were consistent with the analytical solutions to the original problem. In conclusion, the numerical examinations successfully verified the validity of the error estimation technique. We successfully created an error estimation scheme with a high predictive capability.

Acknowledgment: The authors are grateful to the Ministry of Science and Technology of Taiwan for financial support (grant number MOST-07-2221-E-197-008-**)**.

Conflicts of Interest: The authors declare that they have no conflicts of interest to report regarding the present study.

References

Alves, C. J. S. (2009): On the choice of source points in the method of fundamental solutions. *Engineering Analysis with Boundary Elements*, vol. 33, no. 12, pp. 1348-1361.

Atluri, S. N. (2004): *The Meshless Local Petrov-Galerkin (MLPG) Method for Domain & BIE Discretizations*. Tech Science Press.

Atluri, S. N.; Zhu, T. (1998): A new meshless local Petrov-Galerkin (MLPG) approach in computational mechanics. *Computational Mechanics*, vol. 22, no. 2, pp. 117-127.

Atluri, S. N.; Shen, S. (2002): The meshless local Petrov-Galerkin (MLPG) method: a simple & less-costly alternative to the finite element and boundary element methods. *Computer Modeling in Engineering & Sciences*, vol. 3, no. 1, pp. 11-52.

Chen, J. T.; Chang, M. H.; Chen, K. H.; Lin, S. R. (2002): The boundary collocation method with meshless concept for acoustic eigenanalysis of two-dimensional cavities using radial basis function. *Journal of Sound and Vibration*, vol. 257, no. 4, pp. 667-711.

Chen, J. T.; Chen, I. L.; Chen, K. H.; Lee, Y. T.; Yeh, Y. T. (2004): A meshless method for free vibration analysis of circular and rectangular clamped plates using radial basis function. *Engineering Analysis with Boundary Elements*, vol. 28, no. 5, pp. 535-545.

Chen, K. H.; Chen, J. T. (2014): Estimating the optimum number of boundary elements by error estimation in a defined auxiliary problem. *Engineering Analysis with Boundary Elements*, vol. 39, no. 2, pp. 15-22.

Chen, K. H.; Chen, J. T.; Kao, J. H. (2008): Regularized meshless method for antiplane shear problems with multiple inclusions. *International Journal for Numerical Methods in Engineering*, vol. 73, no. 9, pp. 1251-1273.

Chen, K. H.; Kao, J. H.; Chen, J. T.; Young, D. L.; Lu, M. C. (2006): Regularized meshless method for multiply-connected-domain Laplace problems. *Engineering Analysis with Boundary Elements*, vol. 30, no. 10, pp. 882-896.

Chen, W.; Gu, Y. (2012): An improved formulation of singular boundary method. *Advances in Applied Mathematics and Mechanics*, vol. 4, no. 5, pp. 543-558.

Chen, W.; Lin, J.; Wang, F. (2011): Regularized meshless method for nonhomogeneous problems. *Engineering Analysis with Boundary Elements*, vol. 35, no. 2, pp. 253-257.

Huang, C. S.; Lee, C. F.; Cheng, A. H. D. (2007): Error estimate, optimal shape factor, and high precision computation of multiquadric collocation method. *Engineering Analysis with Boundary Elements*, vol. 31, no. 7, pp. 614-623.

Karageorghis, A.; Lesnic, D. (2009): Detection of cavities using the method of fundamental solutions. *Inverse Problems in Science and Engineering*, vol. 17, no. 6, pp. 803-820.

Liu, C. S. (2008): Improving the ill-conditioning of the method of fundamental solutions for 2D Laplace equation. *Computer Modeling in Engineering & Sciences*, vol. 28, no. 2, pp. 77-94.

Liu, Q. G.; Sarler, B. (2013): Non-singular method of fundamental solutions for two-dimensional isotropic elasticity problems. *Computer Modeling in Engineering & Sciences*, vol. 91, no. 4, pp. 235-266.

Reutskiy, S. Y. (2005): The method of fundamental solutions for eigenproblems with Laplace and biharmonic operators. *Computers, Materials & Continua*, vol. 2, no. 3, pp. 177-188.

Song, R.; Chen, W. (2009): An investigation on the regularized meshless method for irregular domain problems. *Computer Modeling in Engineering and Sciences*, vol. 42, no. 1, pp. 59-70.

Young, D. L.; Chen, K. H.; Lee, C. W. (2005): Novel meshless method for solving the potential problems with arbitrary domain. *Journal of Computational Physics*, vol. 209, no. 1, pp. 290-321.

Young, D. L.; Chen, K. H.; Lee, C. W. (2006): Singular meshless method using double layer potentials for exterior acoustics. *Journal of the Acoustical Society of America*, vol. 119, no. 1, pp. 96-107.

Young, D. L.; Chen, K. H.; Chen, J. T.; Kao, J. H. (2007): A modified method of fundamental solutions with source on the boundary for solving Laplace equations with circular and arbitrary domains. *Computer Modeling in Engineering & Sciences*, vol. 19, no. 3, pp. 197-222.

Young, D. L.; Chen, K. H.; Liu, T. Y.; Shen, L. H.; Wu, C. S. (2009): Hypersingular meshless method for solving 3D potential problems with arbitrary domain. *Computer Modeling in Engineering & Sciences*, vol. 40, no. 3, pp. 225-270.

Zhang, L.; Li, Z C.; Wei, Y.; Chiang, J. Y. (2013): Cauchy problems of Laplace's equation by the methods of fundamental solutions and particular solutions. *Engineering Analysis with Boundary Elements*, vol. 37, no. 4, pp. 765-780.